Food & Function

Accepted Manuscript

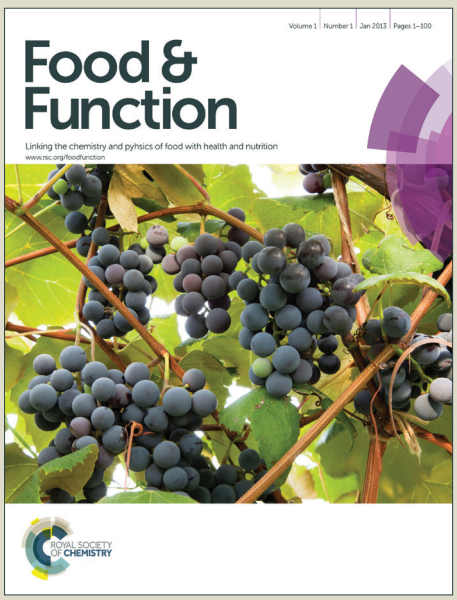

This is an *Accepted Manuscript*, which has been through the Royal Society of Chemistry peer review process and has been accepted for publication.

Accepted Manuscripts are published online shortly after acceptance, before technical editing, formatting and proof reading. Using this free service, authors can make their results available to the community, in citable form, before we publish the edited article. We will replace this *Accepted Manuscript* with the edited and formatted *Advance Article* as soon as it is available.

You can find more information about *Accepted Manuscripts* in the Information for Authors.

Please note that technical editing may introduce minor changes to the text and/or graphics, which may alter content. The journal's standard Terms & Conditions and the Ethical guidelines still apply. In no event shall the Royal Society of Chemistry be held responsible for any errors or omissions in this *Accepted Manuscript* or any consequences arising from the use of any information it contains.

ROYAL SOCIETY OF CHEMISTRY

www.rsc.org/foodfunction

Non-targeted ^{1}H-NMR-metabolomics suggest the induction of master regulators of energy metabolism in the liver of vitamin E-deficient rats

Ali A. Moazzami,[1] Sonja Frank,[2] Antonin Gombert,[1] Nadine Sus,[3] Banu Bayram,[2] Gerald Rimbach,[2] Jan Frank[2,3]

[1]Department of Chemistry and Biotechnology, Swedish University of Agricultural Sciences, P.O. Box 7015, SE-75007, Uppsala, Sweden.

[2]Institute of Human Nutrition and Food Science, Christian-Albrechts-University, D-24118 Kiel, Germany

[3]Institute of Biological Chemistry and Nutrition, University of Hohenheim, D-70599 Stuttgart, Germany

Correspondence:

NMR Metabolomics: Associate Professor Ali A. Moazzami, PhD; Department of Chemistry and Biotechnology, Metabolomics platform, Swedish University of Agricultural Sciences, Box 7015, SE-750 07 Uppsala, Sweden, phone +46-18-672048, email: ali.moazzami@slu.se

Animal model: Professor Jan Frank, PhD; Institute of Biological Chemistry and Nutrition, University of Hohenheim, Garbenstr. 28, D-70599 Stuttgart, Germany, phone: +49-711-459 24459, fax: +49-711-459 23386, email: jan.frank@nutres.de, URL: www.nutrition-research.de

Abstract

The essential function of vitamin E in vivo is not fully understood. Several studies addressed changes in the pattern of gene expression induced by vitamin E, but often did not investigate if these changes altered biochemical pathways and are eventually translated into biological function. We therefore used ^{1}H-NMR metabolomics to investigate the biochemical effects in the liver of rats caused by long-term feeding with diets deficient (dVE; α-tocopherol (αT), <1; γ-tocopherol (γT), <1; all values in mg/kg diet), marginal (mVE; αT, 6; γT, 11), sufficient (sVE; αT, 12; γT, 24), or fortified with vitamin E (fVE; αT, 140; γT, 24). The concentrations of four polar hepatic metabolites were affected by the vitamin E content of the diet; glucose was lower and creatine, phosphocholine, and betaine were higher in deficient compared with rats receiving vitamin E. To achieve further biochemical insight, we investigated transcriptional changes in genes involved in the regulation of metabolic pathways related to these metabolites. Transcription of PGC1α, PPARα, and PPARγ, transcription factors controlling energy metabolism, was lower and that of the fatty acid translocase CD36 higher in animals fed vitamin E-deficient compared to those fed vitamin E-replete diets. Our data thus indicate that consumption of a vitamin E-deficient diet may alter hepatic energy metabolism in rats.

Keywords: Energy metabolism; Glucose; Liver; Metabolites; NMR metabolomics; Rats; Tocopherols; Vitamin E

1 Introduction

Vitamin E was discovered in 1922 by Herbert M. Evans and Katherine S. Bishop as a dietary factor required for foetal development and successful reproduction in rats.[1] A number of deficiency syndromes, such as muscular dystrophy and neuronal dysfunction, were described in subsequent years.[2] Toward the end of the 1930s, the in vitro antioxidant activity of vitamin E was discovered[3] and for the following decades assumed to be its major in vivo-function.[4] Other biological activities of vitamin E, including roles in cell signalling, gene expression, immune response, and apoptosis, have been described more recently (reviewed in [5, 6]). To this day, more than 90 years after the discovery of vitamin E,[1] no specific biochemical function that explains the essentiality of this micronutrient has been described.

Vitamin E is not a single entity, but comprises the eight naturally occurring and structurally related substances α-, β-, γ-, and δ-tocopherol and α-, β-, γ-, and δ-tocotrienol,[5, 7] of which α-tocopherol (αT) is the predominant vitamin E congener and the major lipid-soluble antioxidant in humans.[8] Vitamin E is absorbed together with other lipids in the small intestine, packaged into chylomicrons and transported via the lymph and the portal vein to the systemic circulation from where it is taken up into the liver. The liver preferentially metabolizes the non-αT congeners to side-chain truncated water-soluble carboxyethyl hydroxychromanols, which are eliminated via the bile and urine, and secretes predominantly αT and to a lesser degree γT into the bloodstream.[9, 10] Thus, the liver is the central organ for vitamin E turnover.

A number of studies reported changes in the pattern of gene expression induced by vitamin E,[11-13] but did not investigate if the changes in mRNA expression affected biochemical pathways and were eventually translated into function. Using a metabolomics approach, we have previously observed a shift in the profile of metabolites in response to vitamin E-deficiency in rats.[14]

In the present study, we used ^{1}H-NMR-based metabolomics to investigate the biochemical consequences of long-term feeding of deficient, marginal, sufficient or high dietary concentrations of vitamin E on hepatic metabolism in rats. Using a bottom-up approach, we investigated the pattern of gene expression upstream of the metabolic changes identified by NMR-metabolomics in order to generate new hypotheses that could be tested in independent experiments to uncover the essential biological function of vitamin E.

2 Material and Methods

2.1 Experimental animals, diets, and study design

The animal experiment was performed in accordance with the guidelines for the care and use of animals for experimental procedures and approved by the Ministry of Agriculture, Environment and Rural Areas of the state of Schleswig-Holstein (Germany). Other aspects of this feeding trial and details regarding the preparation of the experimental diets and animal performance were previously published.[15, 16] Briefly, 32 male Fisher 344 rats (Charles River Laboratories, Sulzfeld, Germany) with a mean initial body weight of 51 ± 5 g (mean ± SD) were randomly divided into four groups of eight animals each and fed a vitamin E-deficient (dVE; αT, <1; γT, <1; all values in mg/kg diet), vitamin E-marginal (mVE; αT, 6; γT, 11), vitamin E-sufficient (sVE; αT, 12; γT, 24), or vitamin E-fortified (fVE; αT, 140; γT, 24) experimental diet (ssniff Spezialdiäten GmbH, Soest, Germany) for 6 months. The concentrations and αT and γT compositions of the diets were chosen to mimic a deficient, marginal, and sufficient dietary intake of vitamin E from vegetable oils, where the ratio of αT to γT would be identical, and the use of dietary supplements (which consist of αT only), which would increase αT intake only. The composition of the semi-synthetic diet was as follows (g/kg diet): casein, 240; maize starch, modified, 480; glucose, 110; cellulose, 50; VE-free vitamin premix (E15313-2), 10; mineral premix (E15000), 60; rapeseed oil, 50; all vitamin E in the four diets originated from the respective (vitamin E-stripped, native, or a mix of stripped and native) rapeseed oils used [15]. The rats were housed in Macrolon III cages in a conditioned room (22 ± 2 °C, 55 % relative humidity, 12 h light/dark cycle) and had free access to tap water and the experimental diets. After the 6-month feeding period, the rats were fasted for 12 h prior to CO_2-anaesthesia and decapitation. The liver was excised, snap-frozen in liquid nitrogen, and stored at -80 °C until extraction.

77 **2.2 Liver extraction**

78 Rat liver samples were extracted using a method already described with slight modification.[14]
79 In brief, liver samples (about 100 mg) were homogenized for 1 min in ice-cold methanol-
80 chloroform (2:1, v/v, 3 mL) using a Heidolph Diax 600 homogenizer (Schwabach, Germany).
81 Samples were then sonicated for 30 min and, after the addition of 1 mL ice-cold water and
82 1 mL ice-cold chloroform, vortexed for 1 min, and centrifuged at 4000 × g for 20 min (to
83 allow phase separation). The aqueous supernatant (2.1 mL out of 3 mL polar phase) was then
84 collected, dried using an evacuated centrifuge (Savant, SVC 100H, Savant Instruments INC,
85 New York, NJ, USA) and reconstituted by adding 550 µL of sodium phosphate buffer
86 (0.25 M, pH 7.0) and 30 µL of internal standard solution (1 mM sodium-3-(trimethylsilyl)-
87 2,2,3,3-tetradeuteriopropionate (TSP); Cambridge Isotope Laboratories, Andover, MA, USA),
88 and 40 µL of D_2O, before NMR analysis.

89 **2.3 NMR metabolomics of polar liver extracts**

90 All NMR analyses of liver extracts were performed on a Bruker spectrometer operating at 400
91 MHz equipped with auto-sampler. ^{1}H NMR spectra of liver samples were acquired using the
92 zgesgp pulse sequence (Bruker Spectrospin Ltd.) at 25˚C with 400 scans and 32,768 data
93 points over a spectral width of 6410.25 Hz. Acquisition time was 2.55 s, and relaxation delay
94 was 3.0 s (Fig. 1). NMR signals were identified primarily using the NMR Suite 6.1 library
95 (Chenomx Inc., Edmonton, Canada), Human Metabolome Data Base, Biological Magnetic
96 Resonance Data Bank, or spiking with authentic standard, and were confirmed with 2D NMR
97 in the event of multiplicity.
98 The spectral data were processed using Bruker Topspin 1.3 software and were Fourier-
99 transformed after multiplication by a line broadening of 0.3 Hz and referenced to TSP at 0.0
100 ppm. Spectral phase and baseline were corrected manually. Each spectrum was integrated

using Amix 3.7.3 (Bruker BioSpin GmbH, Rheinstetten) into 0.01 ppm integral regions (buckets) between 0.5-9.5 ppm in which areas between 4.45-5.35 ppm containing residual water were removed (total of 810 buckets). Each spectral region was then normalized to the intensity of internal standard (TSP), which insures the generation of semi-quantitative data after adjusting for the weight of liver sample extracted.

2.4 Hepatic glutathione and glutathione disulfide

Hepatic glutathione and glutathione disulfide were quantified by a published method[17], with modifications. HPLC-grade solvents, perchloric acid, EDTA, and phosphoric acid were purchased from Carl Roth GmbH (Karlsruhe, Germany). Sodium dihydrogen phosphate, 1-octanesulfonic acid and glutathione (G6529, 98-100 % pure; CAS no. 70-18-8) and glutathione disulfide (G4376, 98 % pure; CAS no. 27025-41-8) standards were from Sigma-Aldrich (Steinheim, Germany). Liver tissue (200 mg) was thawed on ice and placed in a 2 mL microcentrifuge tube. One mL ice-cold 10% perchloric acid solution (0.4 N perchloric acid; 100 nM EDTA) was added and samples were sonicated three times for 15 s each. The homogenates were centrifuged (24500 × g, 4 °C, 15 min) and 100 µL supernatant was transferred to an HPLC vial, diluted with 100 µL mobile phase, and 10 µL were injected into a JASCO X-LC HPLC system (autosampler, 3159-AS; two pumps, 3185-PU; solvent mixer, 3180-MX; degasser, 3080-DX; Jasco, Groß-Umstadt, Germany) and detected on an ESA 5600A electrochemical detector equipped with a boron-doped diamond electrode (model 5040; Dionex, Idstein, Germany). Separation of the analytes was achieved on a Reprosil C18 column (5 µm, 250 × 3 mm; Trentec-Analysentechnik, Rutesheim, Germany) using 25 mM sodium dihydrogenphosphate, 1.4 mM 1-octanesulfonic acid, and 6% acetonitrile (adjusted to pH 2.65) as mobile phase at a flow rate of 0.6 mL/min. The potential was set to +1500 mV (vs. a palladium reference electrode) with a clean cell-treatment at +1900 mV for 30 s and a

re-equilibration time of 5 min between injections. Peaks were recorded and integrated with the chromatographic software CoulArray 3.10 (ESA Inc., Chelmsford, MA, USA) and the concentrations of glutathione (GSH) and glutathione disulfide (GSSG) were quantified against authentic external standards.

2.5 Quantification of α-tocopherol in liver tissue

Liver αT concentrations were determined by HPLC with fluorescence detection as previously reported.[18]

2.6 RNA isolation and real-time qRT-PCR

Total RNA was extracted using the RNeasy® Lipid Tissue Protocol (Qiagen) and DNA was digested with the RNase-Free DNase Set (Qiagen). RNA concentrations were determined spectrophotometrically by measuring the absorbance at 260 nm, and RNA purity was determined using the absorption ratio at 260/280 nm with a ratio of 1.6-1.9 considered acceptable. RNA aliquots were stored at -80 °C until PCR analysis. Primer sequences (see Supporting Information Table) for real-time RT-PCR experiments were designed with Primer3 software (version 0.4.0; http://frodo.wi.mit.edu/cgi-bin/primer3/primer3_www.cgi) and primer pairs were obtained from MWG Biotech AG (Ebersberg, Germany). One-step quantitative reverse transcriptase PCR was carried out with the QuantiTec® SYBR® Green RT-PCR kit (Qiagen). Each PCR reaction (final volume 20 μL) contained 0.45 μL of the respective forward and reverse primers, 22.5 μL of QuantiTect®SYBR®Green RT-PCR Master Mix, 0.45 μL QuantiTect RT-Mix, 18.0 μL of RNA dilution and 3.15 μL of water. Real-time PCR amplification was performed in a Rotor-Gene 3000 thermocycler (Corbett Research, Sydney, Australia).

150 **2.7 Quantification of triacylglycerols (TAG), cholesterol and glucose in plasma**

151 TAG, cholesterol and glucose in plasma were measured using the diagnostic kits (OSR61118
152 for TAG, OSR 6116 for cholesterol and OSR 6121 for glucose; Beckman Coulter, Krefeld,
153 Germany) adapted for the Olympus AT200 auto analyzer.

154 **2.8 Statistical analysis of the concentrations of discriminative metabolites in polar liver**
155 **extracts**

156 Principal component analysis (PCA) and orthogonal partial least squares-discriminant
157 analysis (OPLS-DA) were performed using SIMCA-P+ 12.0.1 software (UMETRICS, Umeå,
158 Sweden) after centering and Pareto-scaling of the spectral data as previously described.[14] In
159 the first step of multivariate data analysis, the metabolic profile of the polar phase of liver in
160 each treatment was compared with those in other treatments using separate PCA and OPLS-
161 DA models (total of six comparisons; **Table**) including all 810 spectral buckets generated
162 after binning the NMR spectra between 0.5-9.5 ppm. The NMR signals (Buckets) were
163 identified as discriminating response variable in comparison between each two treatments if
164 their OPLS-DA variable influences on projection (VIP) ≥1 and VIP jackknife-based
165 confidence intervals (95% CI) were not close to or included zero. The presence of outliers
166 was investigated using PCA-Hotelling T^2 Ellipse (95% CI), and the normality of multivariate
167 data was investigated using the normal probability plot of PCA model in each step of
168 multivariate data analysis. The multivariate data were normally distributed. The significance
169 of OPLS-DA model was tested using cross-validated (CV) ANOVA ($P<0.05$). CV-ANOVA
170 is a diagnostic tool for assessing the reliability of OPLS models.[19] The diagnostic is based on
171 an ANOVA assessment of the cross-validatory predictive residuals of an OPLS-DA model.
172 Cross-validated ANOVA tests whether the model has significantly smaller cross-validated
173 predictive residuals than just the variation around the global average.[19]

In order to produce an overall view, the spectral data corresponding to the metabolites including 19 buckets, which were found as discriminative in previous stage after paired comparison of each two treatments, were used to generate new PCA and OPLS-DA models incorporating all four treatments. One rat from the dVE group in the OPLS-DA model and one rat from the fVE group in the PCA model were identified as outliers based on Hotelling T^2 Ellipse (95% CI) and therefore omitted.

The absolute concentrations of the metabolites, which their corresponding NMR signals were found discriminative in OPLS-DA model incorporating all four treatments, were calculated from the NMR spectra using NMR Suite 7.1 profiler (ChenomX Inc, Edmonton, Canada) and internal standard (TSP) after correction for overlapping signals. The absolute concentrations of the discriminative metabolites were further investigated by 1-way ANOVA followed by Tukey multiple comparison test. The absolute concentrations of metabolites were log-transformed before ANOVA, when the distribution was skewed (Anderson-Darling test, $P<0.05$).

3 Results

Body weights of rats fed vitamin E-deficient (dVE; 363±12 g), -marginal (mVE; 367±18 g), -sufficient (sVE; 372±21 g), or -fortified (fVE; 349±21 g) diets for 6 months did not differ significantly at the end of the experiment, as described in detail earlier.[15, 16] No signs of vitamin E-deficiency (ataxia) or other adverse effects were observed after 6 months in animals on the vitamin E-deficient (<1 mg/kg diet) or any of the other diets[15, 16], which is in agreement with previous studies.[14, 20, 21]

The mean concentrations of αT in the liver increased significantly with increasing VE intake (**Figure 1**). The comparisons of the metabolic profiles were performed between each paired treatment groups using separate OPLS-DA models (total of 6

198 comparisons). Metabolites that were found discriminative in each comparison (VIP >1) are
199 presented in **Table**. Twelve metabolites and 5 unknown NMR signals significantly differed in
200 paired comparisons between different treatment groups (**Table**). Next, new PCA (including 8
201 components) and OPLS-DA (including one predictive component and one orthogonal
202 component) models incorporating all four treatments (**Figure 2**) were established using the
203 liver metabolites that were found discriminative at the previous stage (paired comparison)
204 (**Table**). OPLS-DA model parameters for one predictive component were: $R^2X = 0.46$, $R^2Y =$
205 0.33, $Q^2 = 0.32$, CV-ANOVA $p = 0.011$; PCA model parameters were: R^2X first component =
206 0.479, R^2X second component = 0.26**.**

207 Both, the PCA and the OPLS-DA model indicated clear separation of treatment
208 groups along the first component (**Figure 2**). The treatments dVE and fVE were located
209 farthest from each other along the first component indicating the largest metabolic differences
210 (**Figure 2**). Four out of fourteen metabolites, namely glucose, betaine, phosphocholine, and
211 creatine, were found discriminative along the first predictive component of the OPLS-DA.
212 The absolute concentrations of these four metabolites were calculated from the NMR spectra
213 and compared using 1-way ANOVA. There was a significant difference ($P<0.05$) in hepatic
214 glucose, creatine, betaine, and phosphocholine in response to dietary vitamin E (**Figure 1**).

215 Analysis of variance revealed significant differences in hepatic glutathione
216 ($P<0.01$; **Figure 1**), plasma total cholesterol ($P<0.001$), and plasma triacylglycerol (TGA;
217 $P<0.01$; **Figure 3**), and relative hepatic mRNA expression of peroxisome proliferator-
218 activated receptor α (PPARα) ($P<0.01$) and γ (PPARγ; $P<0.001$), peroxisome proliferator-
219 activated receptor gamma coactivator 1-α (PGC1α; $P<0.05$), scavenger receptor/fatty acid
220 translocase CD36 ($P<0.001$), α-tocopherol transfer protein (α-TTP; $P<0.01$), and glucose-6-
221 phosphatase (G6PC; $P<0.01$) (**Figure 4**) between treatments. However, the trend across the
222 treatments did not occur uniformly for the different variables reported above **(Figures 1-4)**.

There were no significant differences in hepatic glutathione disulfide (GSSG), the hepatic GSH/GSSG ratio (Figure 1), plasma glucose **(Figure 3)** and relative hepatic mRNA expression of hypoxia-inducible factor 1-α (HIF1α), sterol regulatory element-binding protein 1 (SREBP1), insulin-like growth factor binding protein 1 (IGFBP1) and 2 (IGFBP2), phosphofructokinase (PFK), fructose-1,6-bisphospatase (FBP), and phosphoenolpyruvate carboxykinase (PCK; data not shown).

4 Discussion

Several cellular functions that may or may not be independent of its antioxidant activity, including the regulation of gene expression and modulation of signalling pathways, have been attributed to vitamin E.[6] In order to elucidate the cellular function(s) of vitamin E, it is important to investigate if events on the level of gene transcription and translation ultimately are converted into a biological activity that is reflected by metabolic changes. Therefore, in the present study, we used a bottom-up metabolomics approach to examine the biochemical effects of increasing dietary doses of vitamin E in a rat model and to investigate the coherence between transcriptional and metabolic effects. We chose the liver as the target tissue, because it is the central organ in vitamin E trafficking and metabolism, and focused on metabolites in the polar phase to reflect the metabolism.

We observed lower glucose concentrations in the liver of rats fed deficient compared with those fed fortified diets (**Figure 1B**), which is consistent with our previous metabolomics study on vitamin E deficiency in rats.[14] There was a positive correlation between glucose and glycogen in the liver (R^2=70.7 %; $P<0.001$). Although the experimental diets dose-dependently increased hepatic αT, liver glucose concentrations did not differ significantly between the dVE, mVE, and sVE groups (**Figure 1B**).

In order to test the notion that lower glucose concentrations in the livers of rats fed vitamin E-deficient diets might be associated with reduced gluconeogenesis during fasting, we measured the relative mRNA expression of PGC1α, which plays a critical role in the maintenance of glucose, lipid, and energy homeostasis.[22, 23] PGC1α, through transcriptional co-activation of glucocorticoid receptors and the hepatic nuclear factor-4α (HNF-4α), activates an entire program of key gluconeogenic enzymes, including phosphoenolpyruvate carboxykinase (PCK) and glucose-6-phosphatase (G6PC).[24, 25] Consistent with this notion, the relative mRNA expression of PGC1α (**Figure 4A**) followed the same pattern as the glucose content in the liver (**Figure 1B**) and was lower in dVE compared with fVE. This is in general agreement with induced PGC1α protein in the brain of guinea pigs orally administered tocotrienol-rich rice bran extract.[26] Furthermore, the PGC1α target gene G6PC was down-regulated in animals fed the vitamin E-deficient diet (**Figure 4F**). PGC1α further modulates lipid/energy metabolism through co-activation of PPARα and PPARγ. Therefore, we measured the relative mRNA expression of these nuclear receptors, which too was lower in the livers of animals fed vitamin E-deficient compared to vitamin E-containing diets. Consistently, PPARγ expression is up-regulated by vitamin E (both αT and γT) in colon cancer cells (SW480)[27], prostate cancer cells[28] and keratinocytes[29]. PGC1α can promote insulin resistance in the liver through PPARα-dependent induction of mammalian tribbles homolog (TRB-3), which is a fasting-inducible inhibitor of the serine-threonine kinase Akt/PKB and insulin signalling.[30] Lower expression of PPARα and PGC1α in the present study may suggest alleviated inhibitory effects of the downstream TRB-3 on insulin signalling when on a vitamin E-deficient diet. Insulin is an inhibitor of gluconeogenesis in the liver. Therefore, reduced hepatic glucose in animals fed the vitamin E-deficient diet might be the result of increased insulin signalling in the liver. Plasma glucose concentrations, however, did not differ between groups (**Figure 3**), which is likely explained by the fact that our

272 animals were fasted for >12 h prior to blood sampling and any differences in postprandial
273 blood glucose were already evened out.

274 We further investigated the metabolic effects of vitamin E on the interplay
275 between glucose and lipid metabolism by measuring other parameters associated with lipid
276 metabolism. Plasma total cholesterol and TAG were lower in animals fed deficient compared
277 with fortified diets (**Figure 3**). Intriguingly, the hepatic mRNA expression of the fatty acid
278 transporter CD36 was higher in the dVE than in the mVE, sVE, and fVE groups (**Figure 4**).
279 These findings are consistent with previous observation in smooth muscle cells and
280 macrophages, where incubation with αT reduced CD36 expression.[31, 32] The increased CD36
281 and reduced PPARα, PPARγ, and PGCα1 in vitamin E-deficiently fed animals may indicate
282 higher fatty acid uptake and lower β-oxidation in their liver. In agreement with this, αT
283 supplementation was recently shown to decrease CD36 expression and TAG accumulation in
284 the liver of guinea pigs.[33] Unfortunately, due to the limited amount of liver tissue available,
285 we were not able to determine hepatic TAG in our rats. The present findings suggest that
286 vitamin E supplementation may reduce hepatic fatty acid uptake via reduced CD36 expression
287 and may increase fatty acid metabolism (indicated by up-regulated expression of PPARα,
288 PPARγ, and PGCα1) and thereby reduce lipid accumulation.

289 An increase in the creatine content of liver was observed in the present
290 experiment, which is consistent with previous findings in the liver of vitamin E-deficient
291 rabbits and mice.[34, 35] Creatine is synthesized mainly in the liver. Its main role is in the
292 creatine kinase/phosphocreatine system as a part of the cell's energy shuttle. The creatine
293 kinase/phosphocreatine energy shuttle, via highly diffusible phosphocreatine and creatine,
294 connects subcellular sites of ATP production (e.g. glycolysis and mitochondrial oxidative
295 phosphorylation) with sub-cellular sites of ATP utilization.[36] Increased creatine in animals on
296 a vitamin E-deficient diet (**Figure 1E**) may indicate changes in energy metabolism and energy

balance that may be consistent with the observed changes in hepatic glucose (**Figure 1B**), and the expression of master regulators of energy metabolism (PGC1α, PPARα, and PPARγ; **Figure 4**). It is important to understand if the increase in hepatic creatine concentrations in dVE is caused by induction of creatine biosynthesis and/or changes in creatine kinase activity. Creatine kinase, the enzyme converting creatine to phosphocreatine, is inactivated by reactive oxygen species,[37] and PGC1α is required for the induction of many ROS-detoxifying enzymes,[38] which may suggest a link between creatine kinase activity and modulated PGC1α expression in the present study. Creatine kinase/phosphocreatine is particularly important in cells with high energy requirements such as those in skeletal muscles, kidney, brain, retina photoreceptor cells, and spermatozoa [39]. Interestingly, vitamin E-deficiency affects predominantly the above-mentioned tissues and deficiency symptoms include muscular dystrophy and neurological dysfunction. This could hint towards a role of impaired energy metabolism in the pathophysiology of vitamin E deficiency.

The use of fasted animals (>12 h) to reduce the impact of recent feed intake on the liver metabolome represents a limitation of our study, since fasting affects energy metabolism. We can therefore not exclude that the vitamin E-dependent differences in the polar liver metabolome in the fasting state may differ from that observed in fed animals, a question deserving further attention in targeted investigations of the liver metabolome in vitamin E-deficient animals.

Conclusions

Using a bottom-up approach to generate novel hypotheses that can be tested independently and may help to understand the essential biological function of vitamin E, we studied the differences in the abundance of polar metabolites in the liver in response to increasing dietary doses of vitamin E. The most important changes observed include a significant decrease in

322 glucose and increase in creatine in the liver of rats maintained for 6 months on a vitamin E-
323 deficient diet. These findings suggest a change in energy metabolism in dietary vitamin E-
324 deficiency, which were consistent with the pattern of expression of master energy regulators.
325 Based on these findings, we propose that the impact of vitamin E-deficiency on the
326 underlying signalling pathways should be studied in adequately designed models to
327 substantiate or refute the importance of vitamin E for cellular energy homeostasis.
328

329 **Acknowledgments**

330 The study was in part funded by a grant (no. 528/051) from the Union zur Förderung von Öl-
331 und Proteinpflanzen e.V. None of the authors has a known conflict of interest.

References

1. H. M. Evans and K. S. Bishop, *Science*, 1922, 56, 650-651.
2. K. E. Mason, *Fed Proc*, 1977, 36, 1906-1910.
3. H. S. Olcott and O. H. Emerson, *J Am Chem Soc*, 1937, 59, 1008-1009.
4. H. Dam, *Experientia*, 1952, 1, 195-213.
5. J. Frank, X. W. Chin, C. Schrader, G. P. Eckert and G. Rimbach, *Ageing research reviews*, 2012, 11, 163-180.
6. G. Rimbach, A. M. Minihane, J. Majewicz, A. Fischer, J. Pallauf, F. Virgli and P. D. Weinberg, *Proc Nutr Soc*, 2002, 61, 415-425.
7. J. Frank and G. Rimbach, *Aktuel Ernaehr Med*, 2009, 34, 131-140.
8. G. W. Burton, A. Joyce and K. U. Ingold, *Lancet*, 1982, 320, 327.
9. J. Frank, *J Plant Physiol*, 2005, 162, 834-843.
10. N. Grebenstein, M. Schumacher, L. Graeve and J. Frank, *Mol Nutr Food Res*, 2014, DOI: 10.1002/mnfr.201300756.
11. J. Frank, S. de Pascual Teresa and G. Rimbach, *Food Sci Technol Bull*, 2006, Functional Foods: 3, 1-12. Available online at: http://books.google.de/books?id=nNr16elQwY12gC&printsec=frontcover&hl=de#v=onepage&q&f=false.
12. L. Barella, P. Y. Muller, M. Schlachter, W. Hunziker, E. Stocklin, V. Spitzer, N. Meier, S. de Pascual-Teresa, A. M. Minihane and G. Rimbach, *Biochim Biophys Acta*, 2004, 1689, 66-74.
13. G. Rimbach, A. Fischer, E. Stoecklin and L. Barella, *Ann N Y Acad Sci*, 2004, 1031, 102-108.
14. A. A. Moazzami, R. Andersson and A. Kamal-Eldin, *NMR in biomedicine*, 2011, 24, 499-505.

15. S. Gaedicke, X. Zhang, P. Huebbe, C. Boesch-Saadatmandi, Y. Lou, I. Wiswedel, A. Gardemann, J. Frank and G. Rimbach, *Br J Nutr*, 2009, 102, 398-406.

16. S. Gaedicke, X. Zhang, C. Schmelzer, Y. Lou, F. Doering, J. Frank and G. Rimbach, *FEBS Lett*, 2008, 582, 3542-3546.

17. H. J. Park, E. Mah and R. S. Bruno, *Anal Biochem*, 2010, 407, 151-159.

18. K. Augustin, R. Blank, C. Boesch-Saadatmandi, J. Frank, S. Wolffram and G. Rimbach, *J Anim Physiol Anim Nutr*, 2008, 92, 705-711.

19. L. Eriksson, J. Trygg and S. Wold, *Journal of Chemometrics*, 2008, 22, 594-600.

20. K. Adachi, M. Izumi and T. Mitsuma, *Neurochem Res*, 1999, 24, 1307-1311.

21. W. P. Burkard, K. F. Gey, H. Weiser and U. Schwieter, *Experientia*, 1968, 24, 807-808.

22. J. Lin, C. Handschin and B. M. Spiegelman, *Cell Metab*, 2005, 1, 361-370.

23. C. Liu and J. D. Lin, *Acta biochimica et biophysica Sinica*, 2011, 43, 248-257.

24. J. C. Yoon, P. Puigserver, G. Chen, J. Donovan, Z. Wu, J. Rhee, G. Adelmant, J. Stafford, C. R. Kahn, D. K. Granner, C. B. Newgard and B. M. Spiegelman, *Nature*, 2001, 413, 131-138.

25. J. Rhee, Y. Inoue, J. C. Yoon, P. Puigserver, M. Fan, F. J. Gonzalez and B. M. Spiegelman, *Proc Natl Acad Sci U S A*, 2003, 100, 4012-4017.

26. S. Hagl, A. Kocher, C. Schiborr, S. H. Eckert, I. Ciobanu, M. Birringer, H. El-Askary, A. Helal, M. T. Khayyal, J. Frank, W. E. Muller and G. P. Eckert, *Pharmacological research : the official journal of the Italian Pharmacological Society*, 2013, 76, 17-27.

27. S. E. Campbell, W. L. Stone, S. G. Whaley, M. Qui and K. Krishnan, *BMC cancer*, 2003, 3, 25.

28. S. E. Campbell, P. R. Musich, S. G. Whaley, J. B. Stimmel, L. M. Leesnitzer, S. Dessus-Babus, M. Duffourc, W. Stone, R. A. Newman, P. Yang and K. Krishnan, *Nutr Cancer*, 2009, 61, 649-662.

29. M. C. De Pascale, A. M. Bassi, V. Patrone, L. Villacorta, A. Azzi and J. M. Zingg, *Arch Biochem Biophys*, 2006, 447, 97-106.

30. S. H. Koo, H. Satoh, S. Herzig, C. H. Lee, S. Hedrick, R. Kulkarni, R. M. Evans, J. Olefsky and M. Montminy, *Nat Med*, 2004, 10, 530-534.

31. R. Ricciarelli, J. M. Zingg and A. Azzi, *Circulation*, 2000, 102, 82-87.

32. A. Azzi, R. Ricciarelli and J. M. Zingg, *FEBS Lett*, 2002, 519, 8-10.

33. M. C. Podszun, N. Grebenstein, A. Spruss, T. Schlueter, C. Kremoser, I. Bergheim and J. Frank, *J Nutr Biochem*, 2014, (in press).

34. M. R. Heinrich and H. A. Mattill, *Journal of Biological Chemistry*, 1949, 178, 911-917.

35. N. K. Sarkar and U. Srivastava, *J Nutr*, 1964, 83, 193-201.

36. T. Wallimann, M. Tokarska-Schlattner and U. Schlattner, *Amino acids*, 2011, 40, 1271-1296.

37. H. Mekhfi, V. Veksler, P. Mateo, V. Maupoil, L. Rochette and R. Ventura-Clapier, *Circulation research*, 1996, 78, 1016-1027.

38. J. St-Pierre, S. Drori, M. Uldry, J. M. Silvaggi, J. Rhee, S. Jager, C. Handschin, K. Zheng, J. Lin, W. Yang, D. K. Simon, R. Bachoo and B. M. Spiegelman, *Cell*, 2006, 127, 397-408.

39. T. Wallimann, M. Wyss, D. Brdiczka, K. Nicolay and H. M. Eppenberger, *Biochem J*, 1992, 281 (Pt 1), 21-40.

Table. Fold-changes in the contents of metabolites in the aqueous phase of rat liver extracts which were affected by the vitamin E content of the diet[1,2]. Class 1, deficient (dVE); class 2, marginal (mVE); class 3, sufficient (sVE); and class 4, fortified (fVE).

Metabolites	*NMR signal*	*Class 1-2*	*Class 1-3*	*Class 1-4*	*Class 2-3*	*Class 2-4*	*Class 3-4*
CH3-	0.88		0.81	0.71	0.77	0.67	
Leucine	0.96	1.15					
Alanine	1.48			1.23			
Glutamine	2.16	1.14			0.83		1.21
Glutamate	2.36				0.81		
Unknown	2.53				0.86		
Unknown	2.55						1.20
Methionine	2.64		0.73				
Creatine	3.04	0.34	0.30	0.32			
Phosphocholine[3]	3.22	0.63		0.40		0.62	
Betaine	3.27	0.75		0.65			

Unknown	3.29					0.91	
Glucose	3.29–3.90	1.31	1.17	1.44	0.84		1.22
Phosphocholine[3]	4.18			0.65		0.79	
Glycogen	5.412	1.55	1.31	1.74			1.32
Inosine[4]	6.11	1.43			0.80	0.83	
NAD/NADP/NADPH	8.30				0.69	0.86	
Unknown	8.31						1.31
Inosine[4]	8.36	1.40			0.81	0.83	

[1]Fold-changes for each pair of comparisons were calculated by dividing the spectral value of the treatment (class) with the higher digit by that with the lower digit (e.g. signal class 3 divided by signal class 2).

[2]Metabolites with VIP > 1 and for which the corresponding jackknife-based 95% confidence intervals were not close to or including zero were considered different between each treatment pairs (VIP: Variable influences on projection).

[3]Two NMR signals of phosphocholine were independently found different between treatments after statistical analysis.

[4]Two NMR signals of inosine were independently found different between treatments after statistical analysis.

Figure 1. Mean α-tocopherol, glucose, phosphocholine, betaine, creatine, glutathione (GSH) and glutathione disulfide (GSSG) concentrations and their ratios in the livers of rats fed a vitamin E-deficient (dVE), -marginal (mVE), -sufficient (sVE), or -fortified (fVE) diet for 6 months. Bars not sharing a common letter are significantly different at $P<0.05$. Error bars indicate standard deviations. Glucose, phosphocholine, betaine, and creatine were quantified by NMR and α-tocopherol and GSH by HPLC.

Figure 2. Score scatter plot of OPLS-DA model generated using fourteen metabolites found different in pair comparison of the metabolic profile of liver after different treatments. Model parameter for one predictive component: $R^2X = 0.46$, $R^2Y = 0.33$, $Q^2 = 0.32$, CV-ANOVA p = 0.011 (**A**). Score scatter plot of PCA model generated using fourteen metabolites found different in pair comparison of the metabolic profile of liver after different treatments. PCA model parameters were R^2X first component 1 = 0.479, R^2X second component = 0.26. 1-deficient (dVE), 2-marginal (mVE), 3-sufficient (sVE), and 4-fortified (fVE) (**B**). Score t[1] (component 1) and score t[2] (component 2) are new variables summarizing the variation of X-variables (the intensity of NMR signals corresponding to metabolites). For the OPLS-DA model, score to[1] (orthogonal component 1) summarizes the variation of X-variable, which is unrelated to treatment. R2X: Fraction of X variation modeled in the component. Q^2: Overall cross-validated fraction of Y (treatment) variation modeled by X for the component. R^2Y: Fraction of Y variation modeled by Y in the component, using the Y model

Figure 3. Mean fasting plasma glucose, total cholesterol, and triacylglycerol (TAG) concentrations of rats fed a vitamin E-deficient (dVE), -marginal (mVE), -sufficient (sVE), or -fortified (fVE) diet for 6 months. Bars not sharing a common letter are significantly different at $P<0.05$. Error bars indicate standard deviations.

Figure 4. Relative hepatic mRNA expression (normalized for the geometric mean of the housekeeping genes 18S rRNA, GAPDH, and β-actin) of PGC1α, CD36, PPARα, PPARγ, αTTP, and G6PC in rats fed a vitamin E-deficient (dVE), -marginal (mVE), -sufficient (sVE), or -fortified (fVE) diet for 6 months. Bars not sharing a common letter are significantly different at $P<0.05$. Error bars indicate standard deviations.

Figure 1

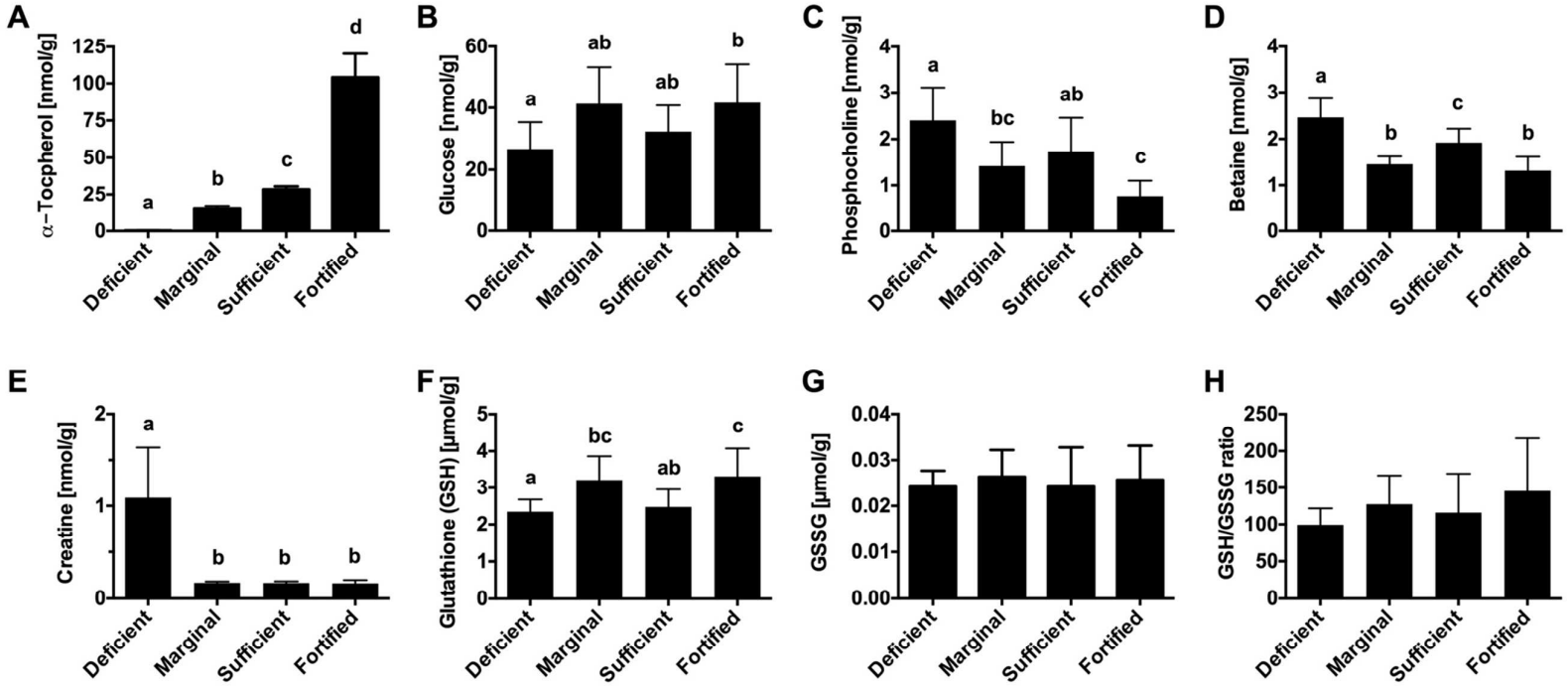

Figure 2

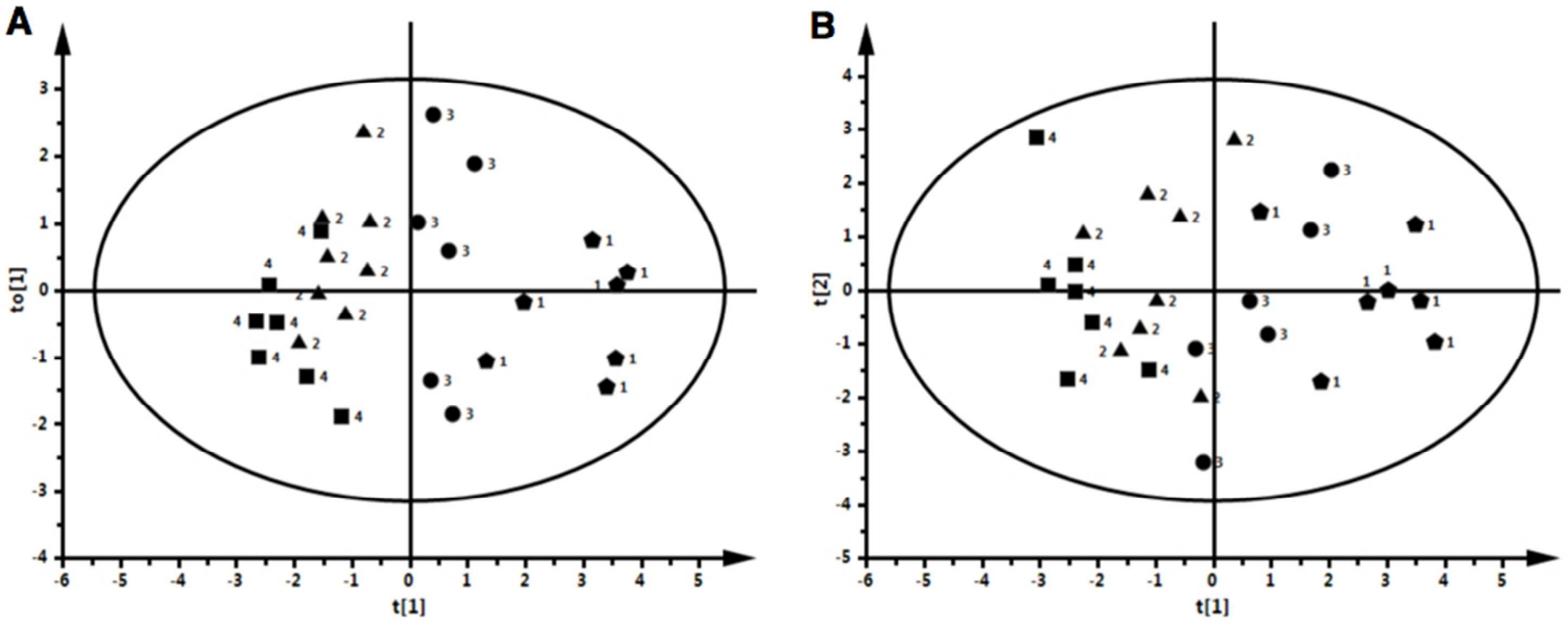

Figure 3

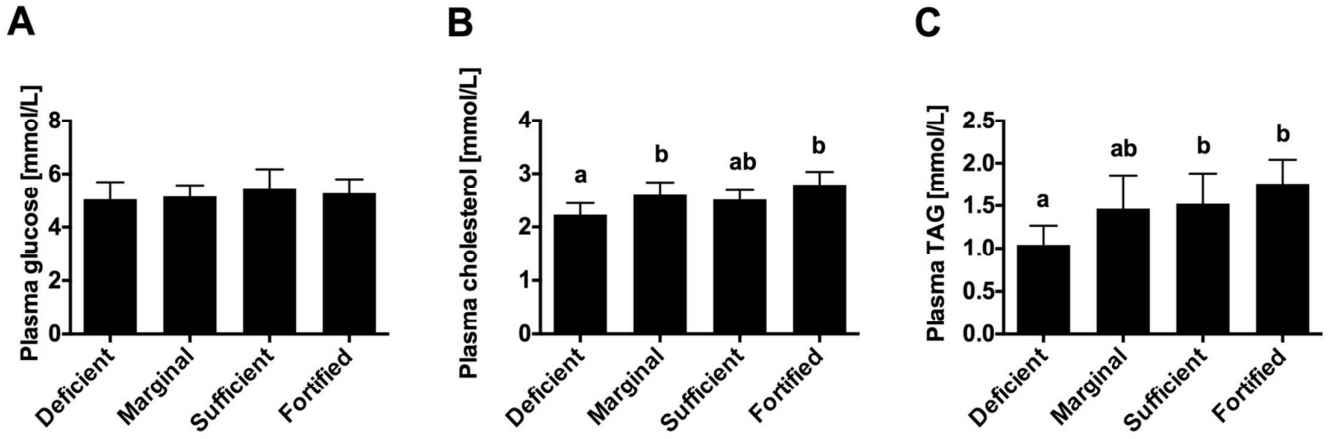

Figure 4